

Supporting information

Terbium Doping LiYbF₄ Nanomaterial-based Scintillator Responding to X-ray with Application of High-resolution Imaging

Xi Chen^{a,b}, Hao Lu^c, Qi Gu^{a,b}, Nan Zhang^{a,b}, Shuaihua Wang^{a,d,}, Shaofan Wu^{a,d}*

a Key Laboratory of Optoelectronic Materials Chemistry and Physics, Fujian Institute
of Research on the Structure of Matter, Chinese Academy of Sciences, Fuzhou

350002, P. R. China

b University of Chinese Academy of Sciences, Beijing 100049, P.R. China

c College of Chemistry and Materials Science, Fujian Normal University, Fuzhou

350117, China

d Fujian Science & Technology Innovation Laboratory for Optoelectronic

Information of China, Fuzhou, Fujian 350108, P. R. China

Fig. S1: Partial TEM image of $\text{LiYbF}_4:15\%\text{Tb}$ NCs, and the crystal quality is good without defects

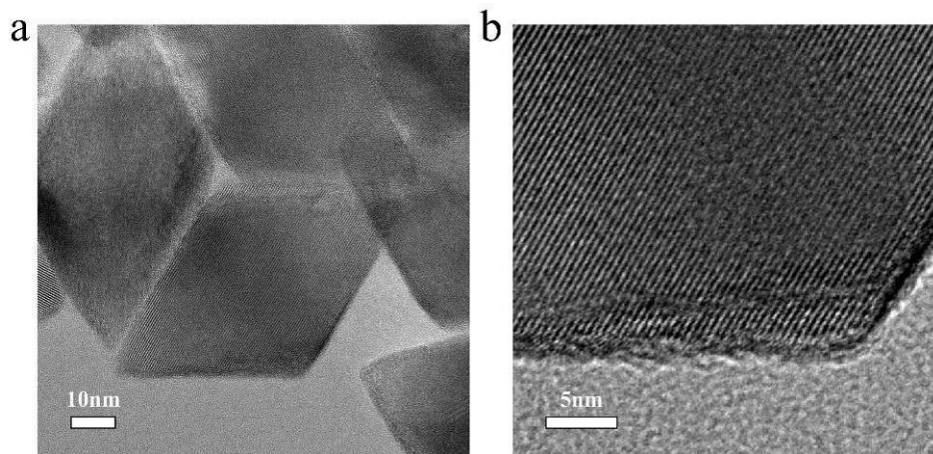


Fig. S2: The fluorescence emission spectrum and excitation spectrum of $\text{LiYbF}_4:15\%\text{Tb}$ NCs

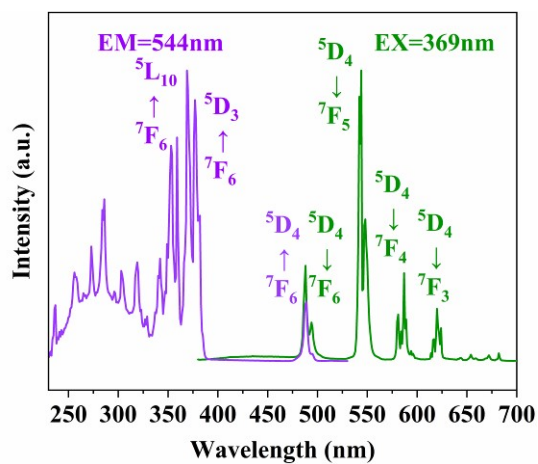


Fig. S3: The energy level transition process of Tb^{3+}

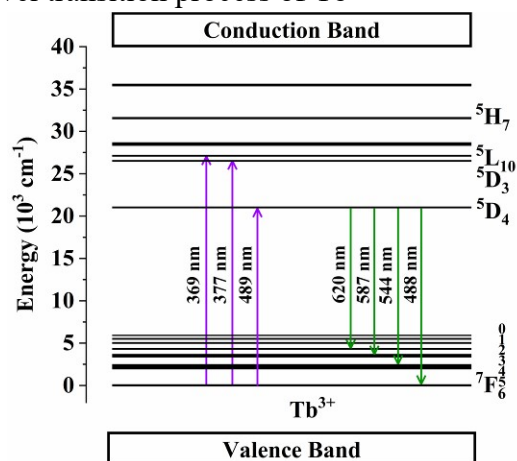


Fig. S4: The radioluminescence spectra of $\text{LiYbF}_4:15\%\text{Tb}$ NCs (a) and BGO (b) at a voltage of 50kV and a dose rate of $8.197\text{mGy/s} \sim 42.29\text{mGy/s}$

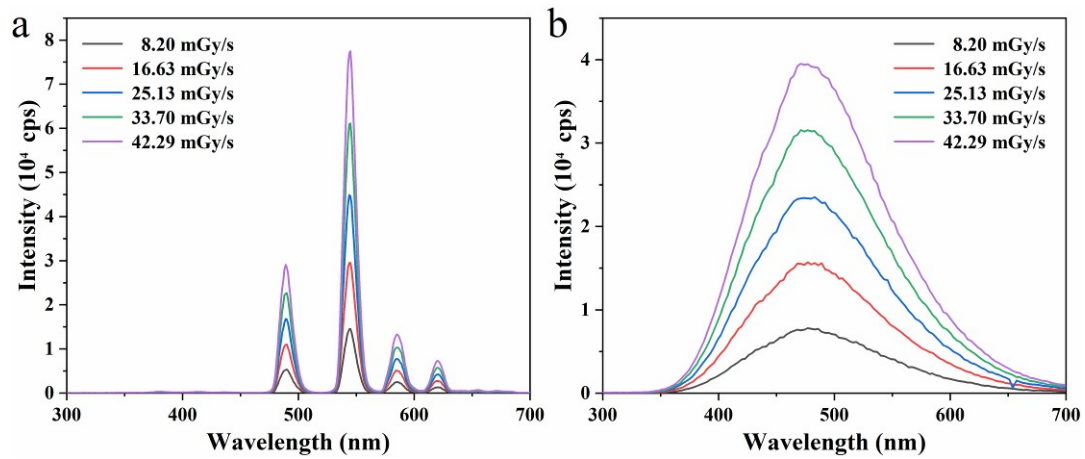


Fig. S5: The XEL of LiYbF₄:15%Tb NCs (a), CsPbBr₃ (b) and BGO (c)

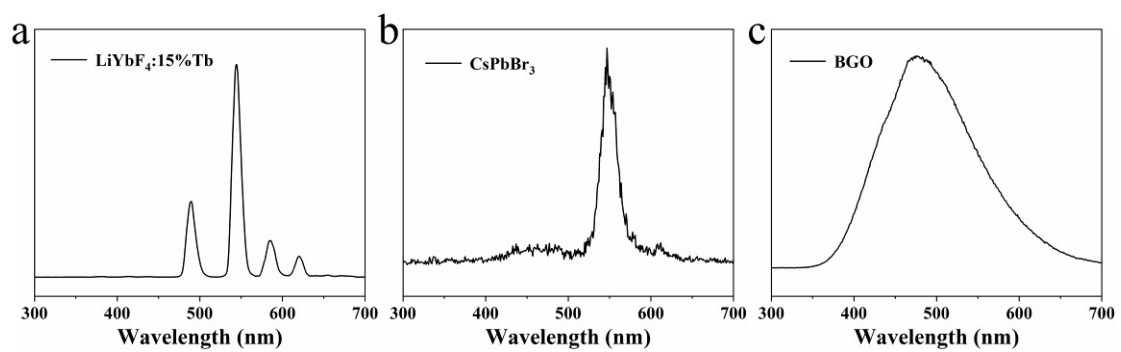


Fig. S6: The TG curve of LiYbF₄:15%Tb NCs ranges from 30-1200°C

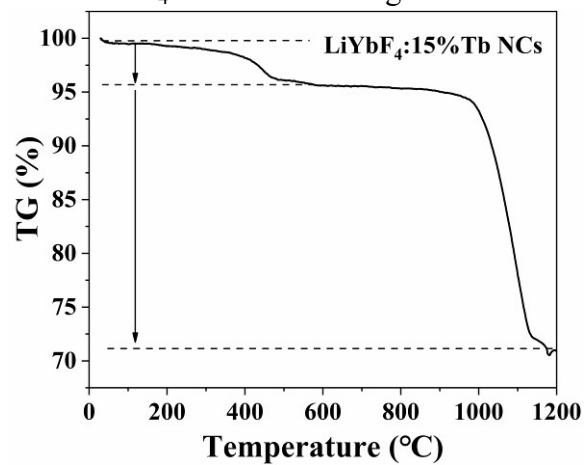


Fig. S7: The changes in the XEL of LiYbF₄:15%Tb NCs after 172 days in the air

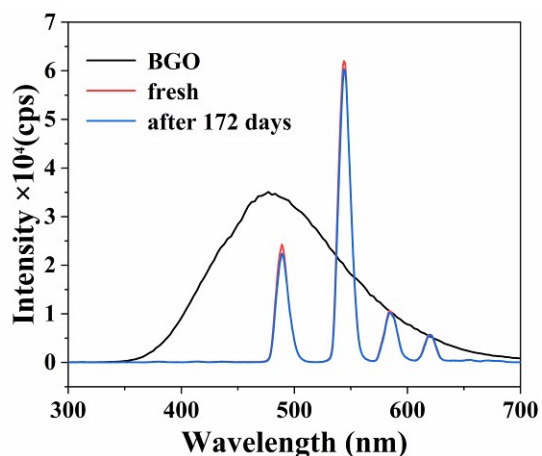


Fig. S8: The physical image of 40wt% LiYbF₄:15%Tb scintillation film

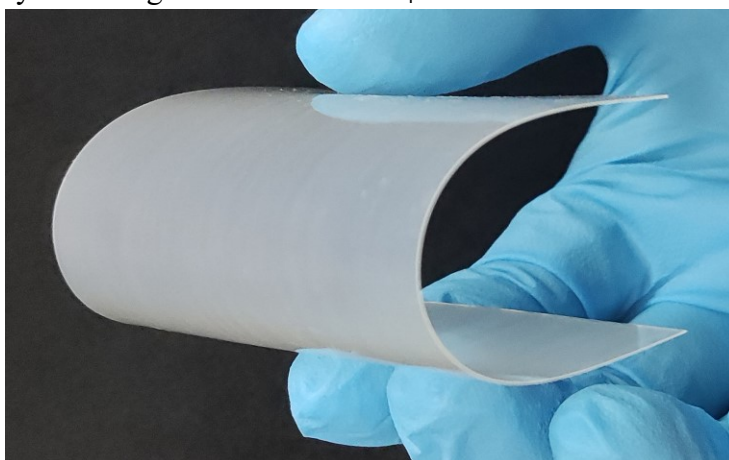


Fig. S9: The radioluminescence spectra of LiYbF₄:15%Tb NCs and LiYbF₄:15%Tb scintillation films at a dose rate of 42.29mGy/s and a voltage of 50kV

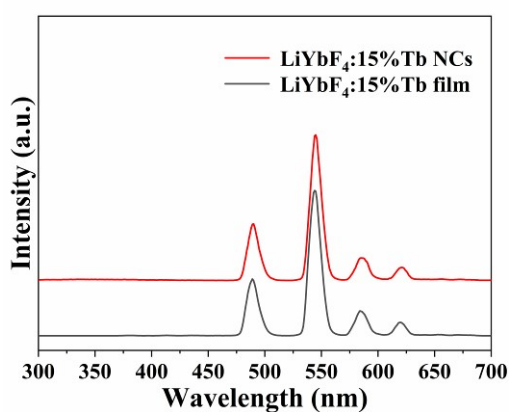


Fig. S10: Physical picture of 0wt%, 10wt%, 20wt%, 30wt%, 40wt% and 50wt% load

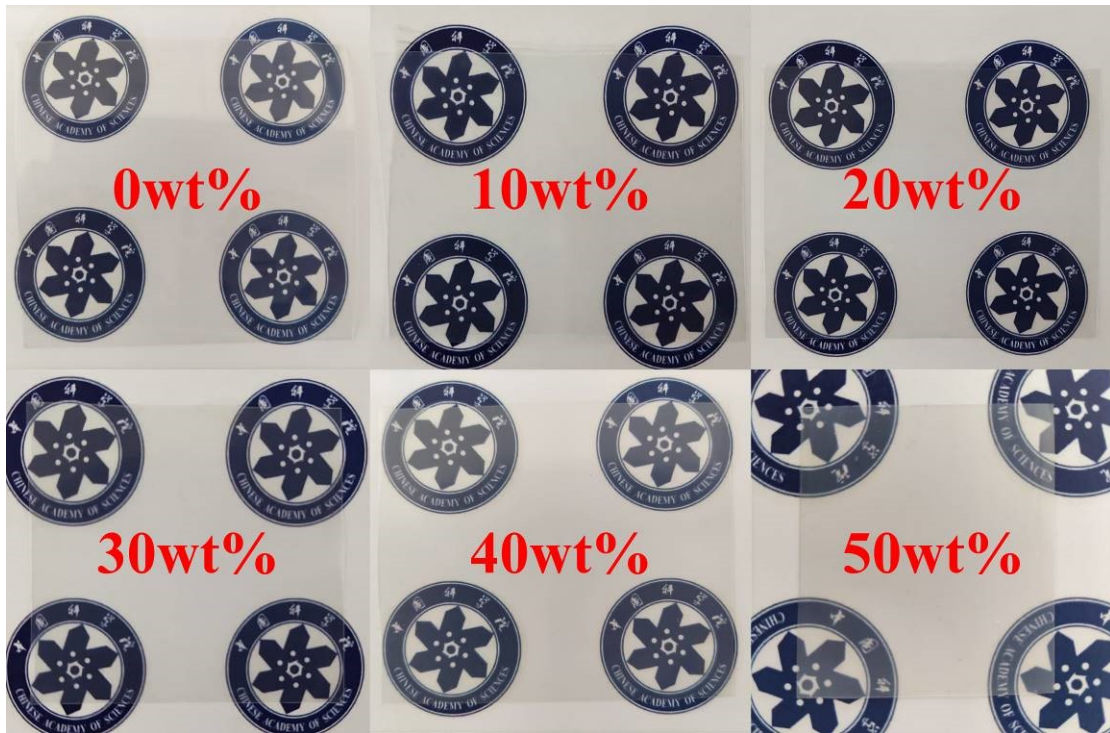


Fig. S11: The physical image of 50wt% $\text{LiYbF}_4:15\%\text{Tb}$ scintillation film under natural light (left) and X-ray (right)

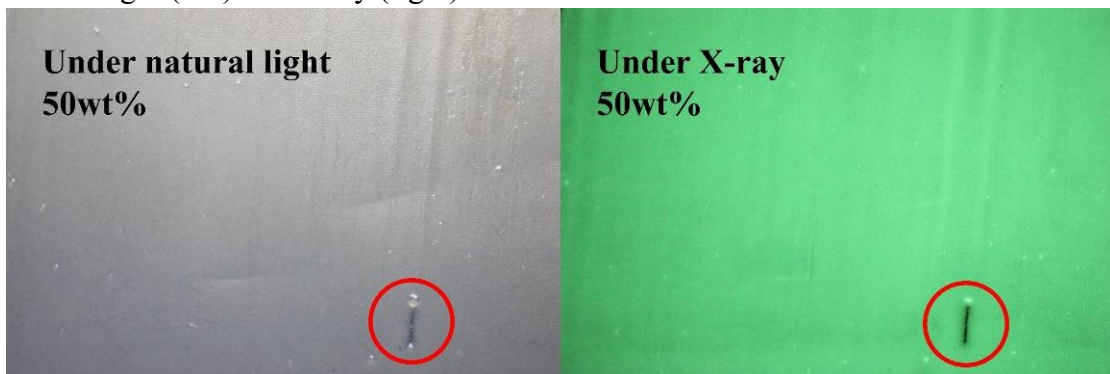


Fig. S12: The stability of the $\text{LiYbF}_4:15\%\text{Tb}$ scintillation film at a dose rate of 12.4mGy/s for 2700s

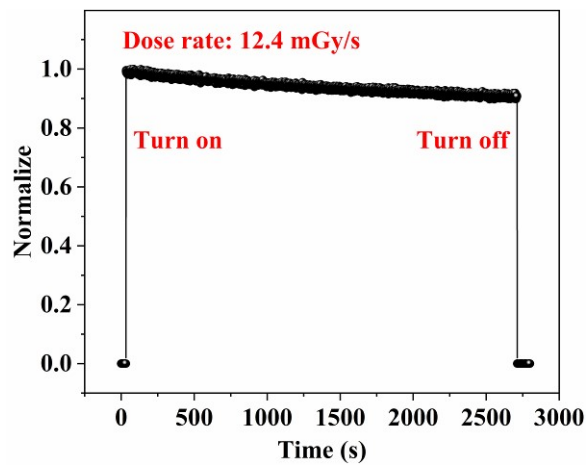


Fig. S13: X-ray imaging system

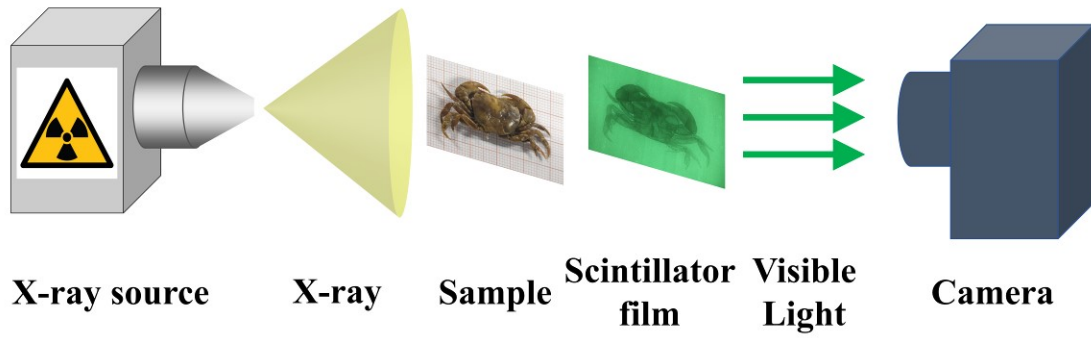


Fig. S14: BGO scintillation film under natural light (left) and X-ray (right)

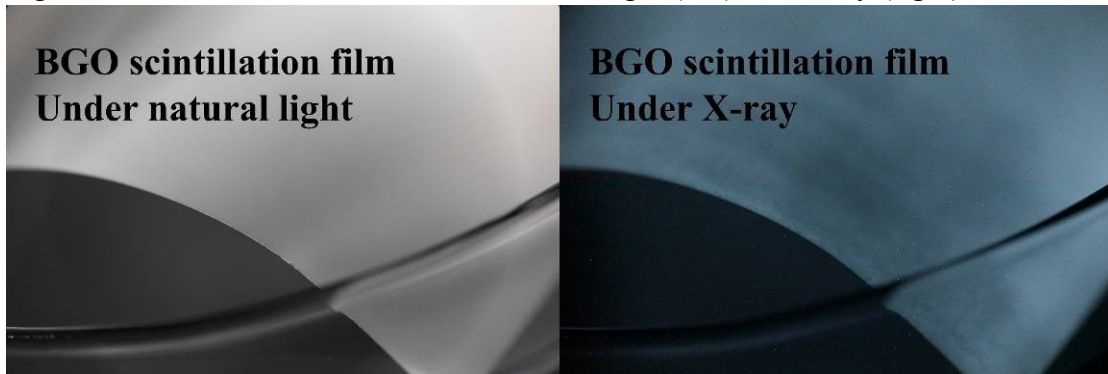


Fig. S15: The grayscale image at 10-20LP/mm of $\text{LiYbF}_4:15\%\text{Tb}$ scintillation film

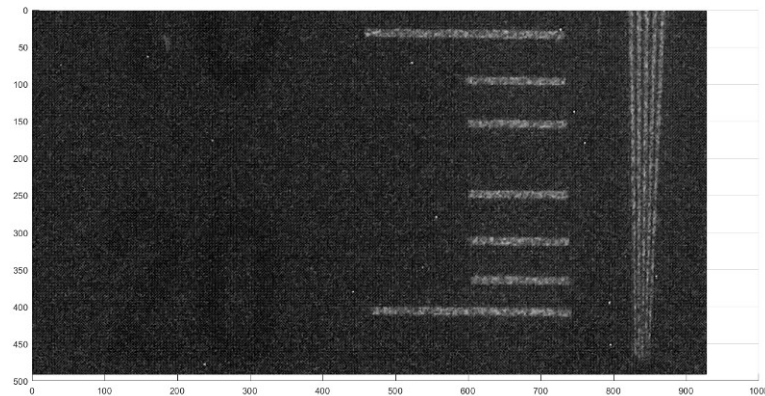


Fig. S16: The grayscale image at 3-10LP/mm of BGO scintillation film

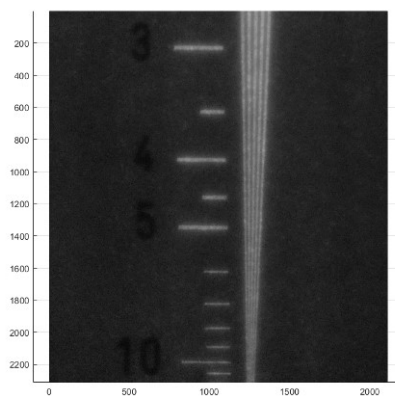


Fig. S17: The stripe brightness extraction map of $\text{LiYbF}_4:15\%\text{Tb}$ scintillation film at

14-20LP/mm. Each peak corresponds to a bright fringe and a trough corresponds to a dark fringe

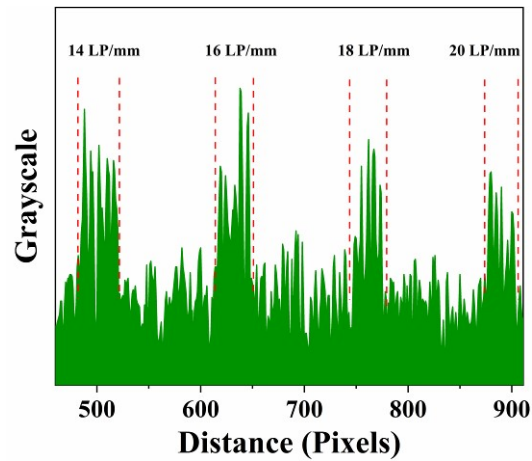


Fig. S18: The stripe brightness extraction map of BGO scintillation film at 4.5-8LP/mm

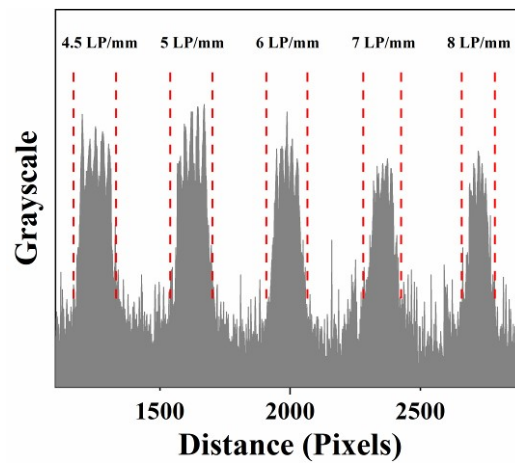


Fig. S19: The X-ray imaging of the data line at a dose rate of 42.29mGy/s and a voltage of 50kV. Metal and plastic are clearly distinguishable in the X-ray image

